Electronic Supplementary Material (ESI) for Nanoscale.
This journal is © The Royal Society of Chemistry 2023

Optimized core-shell lanthanide nanoparticles with ultrabright Ce^{3+}-modulated second near-infrared emission for "lighting" plant

Jikun Wang,[a] Chunsheng Li,[a] Yujie Cui,[a] Qiang Wang,[a] Jin Ye,[a] Jie Yang,[ab] Zhongyuan Liu,[a] Su Zhang,[c] Yujie Fu*[c] and Jiating Xu,*[ab]

[a] Key Laboratory of Forest Plant Ecology, Ministry of Education, College of Chemistry, Chemical Engineering and Resource Utilization, Northeast Forestry University, Harbin 150040, P. R. China

[b] Heilongjiang Provincial Key Laboratory of Ecological Utilization of Forestry-Based Active Substances, Northeast Forestry University, Harbin, 150040, P. R. China

[c] College of Biological Sciences and Technology, Beijing Forestry University, Beijing 100083, P.R. China

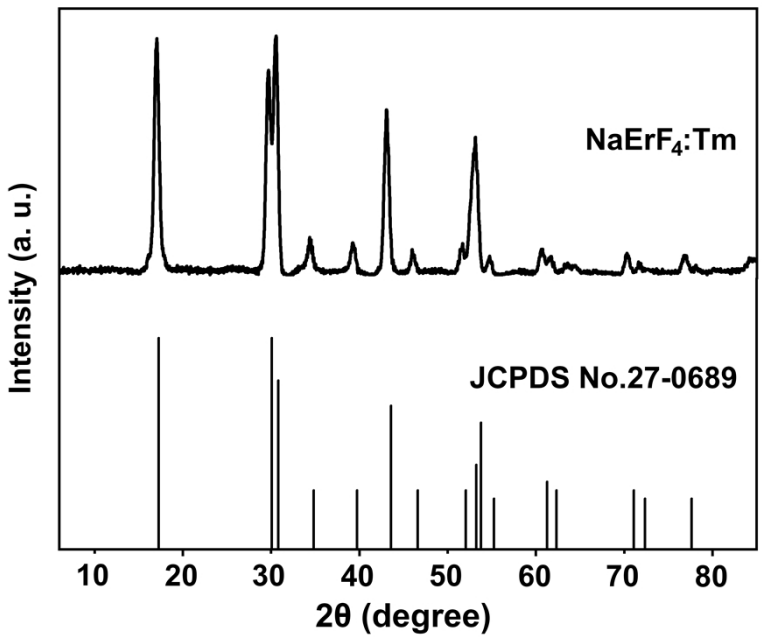

Fig. S1 XRD pattern of the as-synthesized $NaErF_4$:Tm core nanocrystals. All peaks are well indexed in accordance with β-$NaErF_4$ (JCPDS No.27-0689) structure.

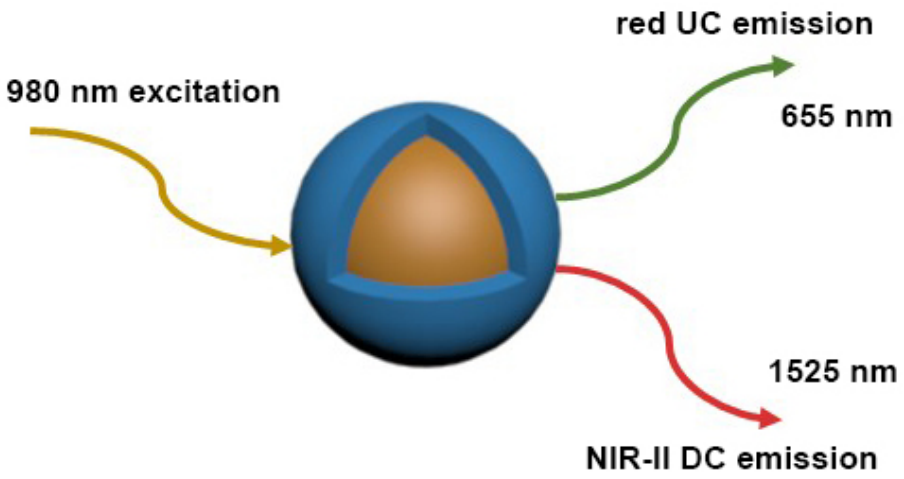

Fig. S2 General depiction of core–active shell $NaErF_4$:Tm@$NaGdF_4$:Yb,Ce nanoparticles showing the absorption of 980 nm light and resulting in red UC and NIR-II DC dual-mode emission.

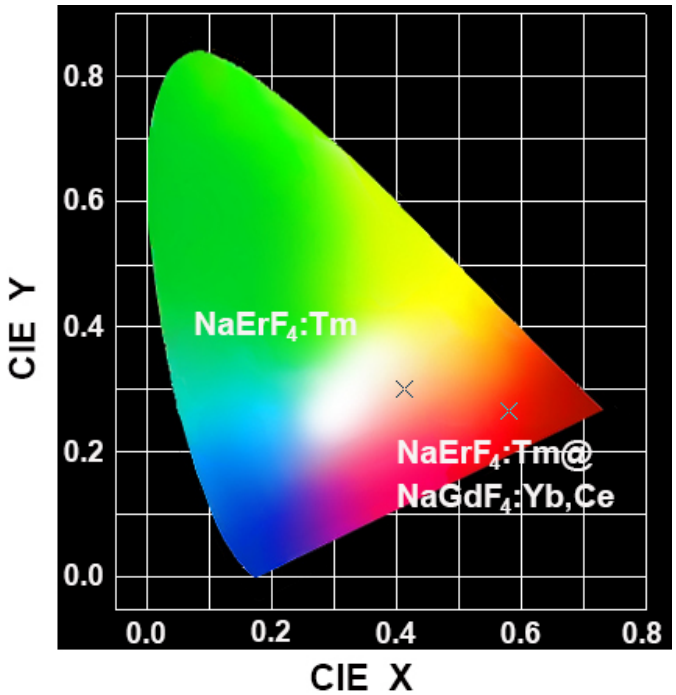

Fig. S3 CIE chromaticity diagrams of $NaErF_4$:Tm core and $NaErF_4$:Tm@$NaGdF_4$:Yb,Ce core-shell nanoparticles.

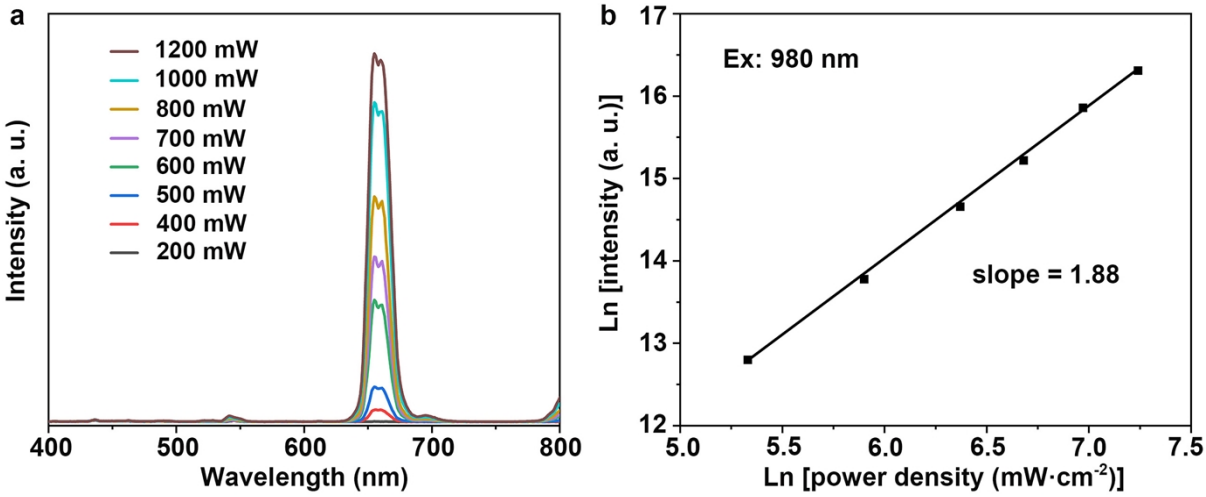

Fig. S4 UC emission spectra of LDNPs under different laser power (a) and pump power dependence of the UC emission in LDNPs (b).

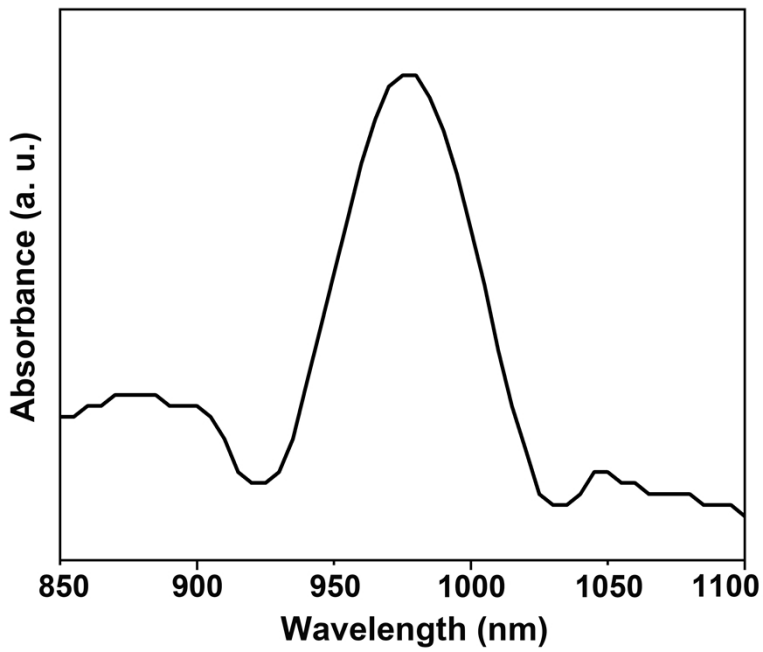

Fig. S5 UV-vis-NIR absorption spectrum of LDNPs.

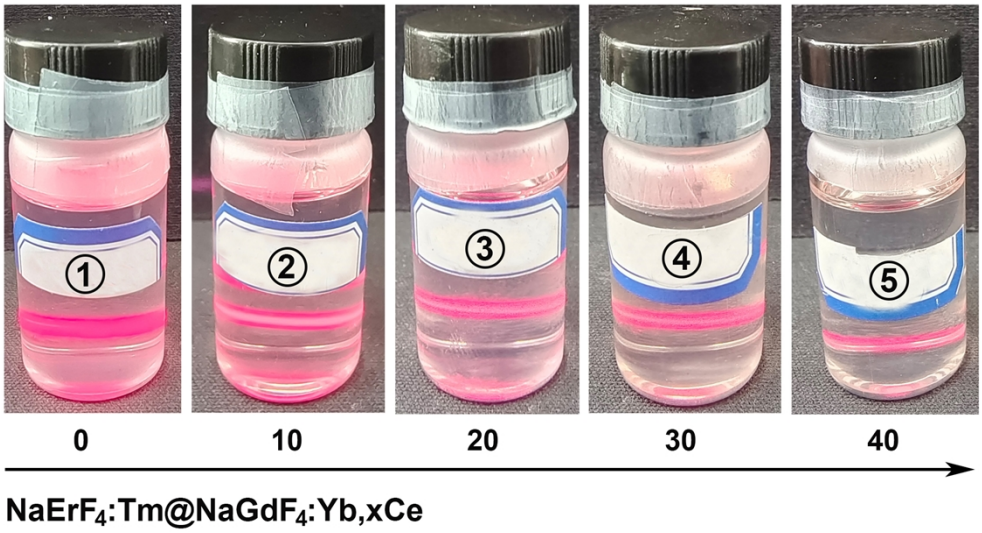

Fig. S6 UC luminescence photographs of $NaErF_4$:Tm@$NaGdF_4$:Yb,xCe (x = 0, 0.1, 0.2, 0.3, 0.4) nanoparticles upon 980 nm laser excitation.

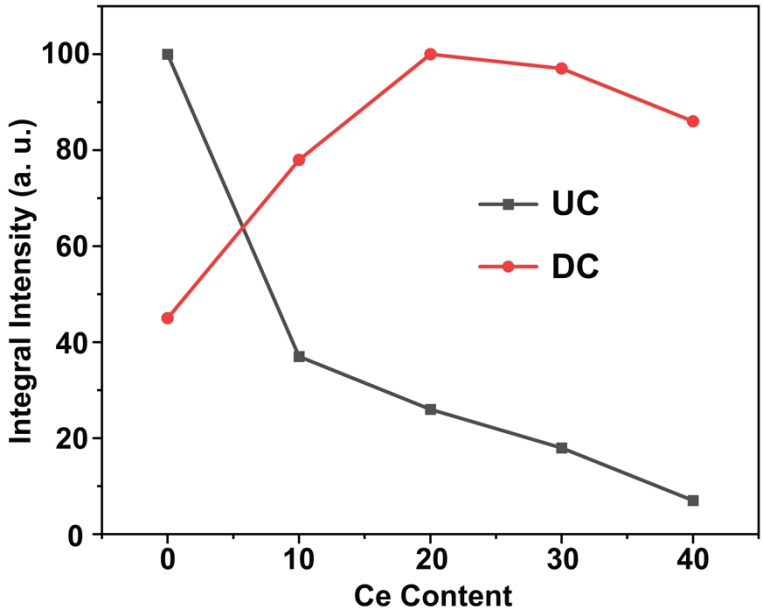

Fig. S7 Corresponding UC/DC integral emission intensity of core-shell nanocrystals with different Ce^{3+} contents.

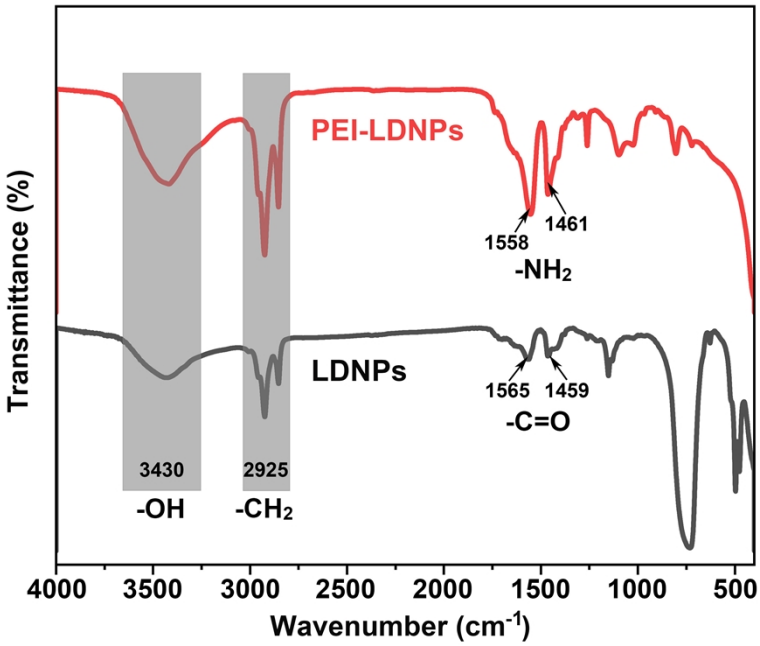

Fig. S8 FT-IR spectra of PEI-LDNPs and LDNPs.

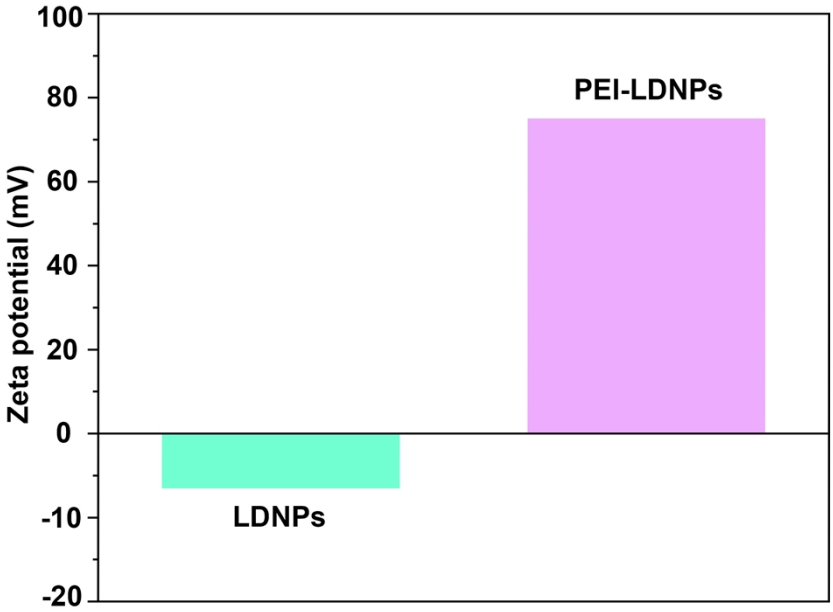

Fig. S9 Zeta potentials of LDNPs and PEI-LDNPs.

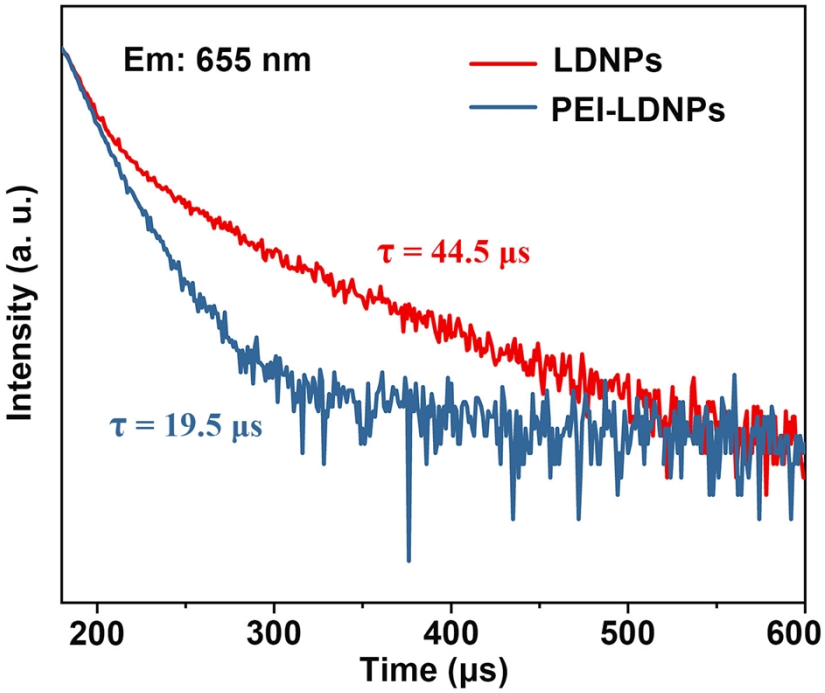

Fig. S10 The lifetime decay curves of LDNPs and PEI-LDNPs detected at 655 nm under 980 nm laser excitation.

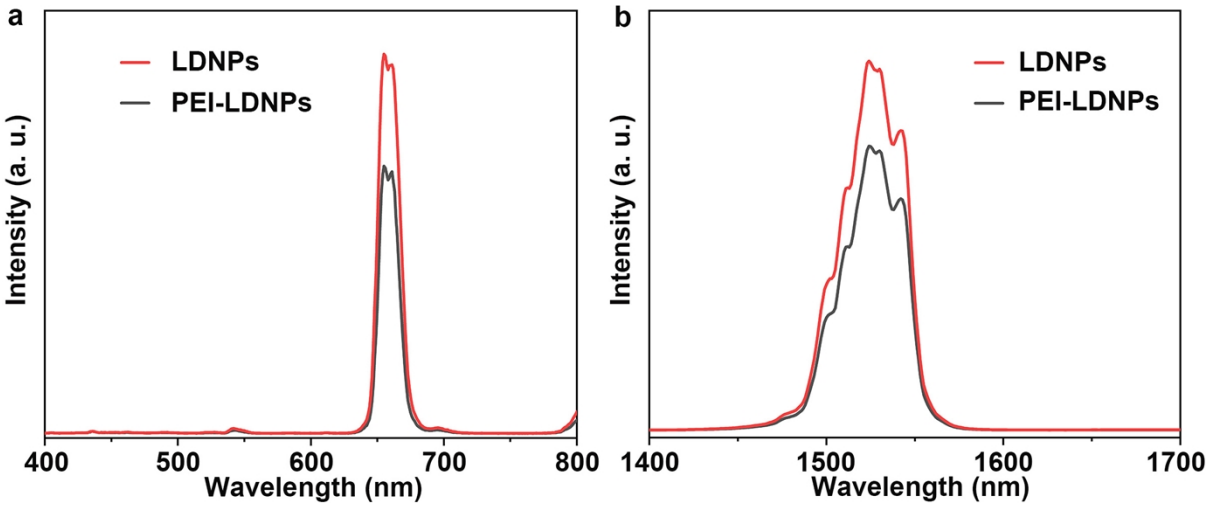

Fig. S11 UC (a) and DC (b) emission spectra of LDNPs and PEI-LDNPs.

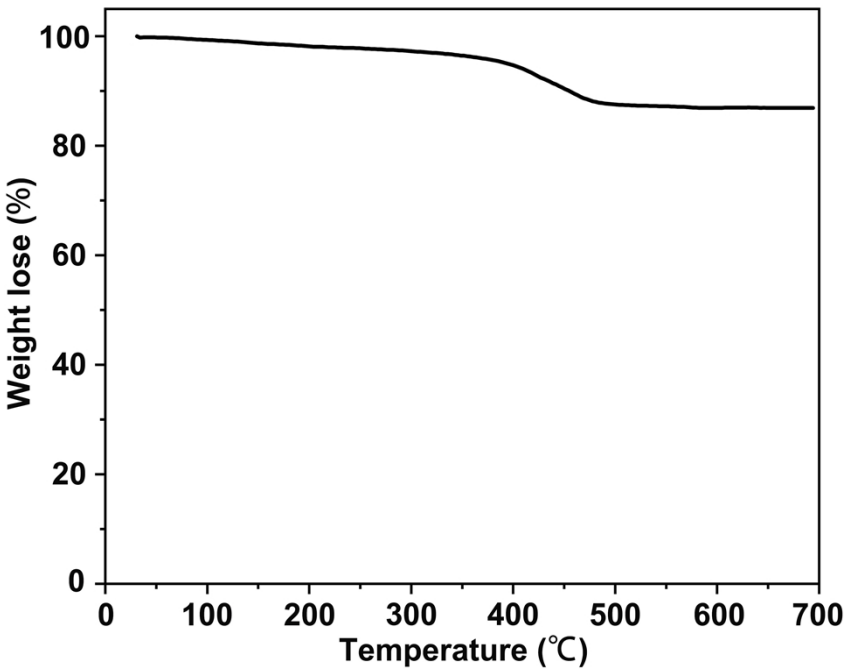

Fig. S12 TGA curve of PEI-LDNPs.

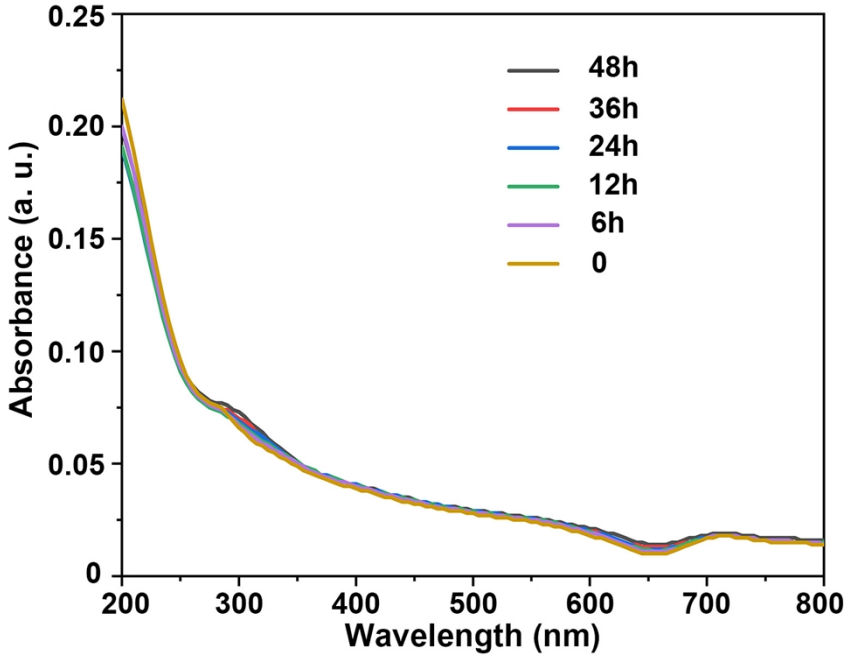

Fig. S13 UV-vis absorbance spectra of the PEI-LDNPs measured at different times.

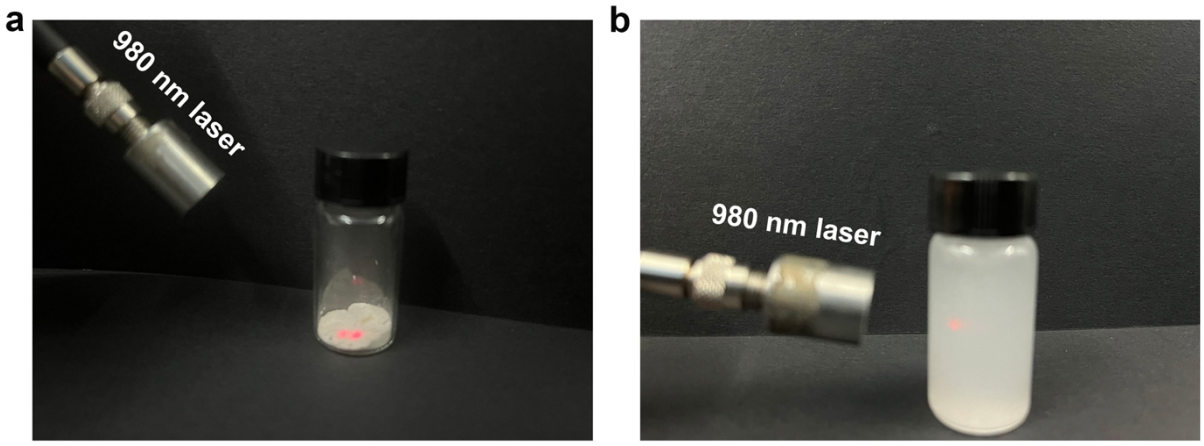

Fig. S14 UC fluorescence photographs of PEI-LDNPs in solid state (a) and dispersed in water (b) upon 980 nm laser excitation.

Fig. S15 Cultivation pictures of *Arabidopsis thaliana*.

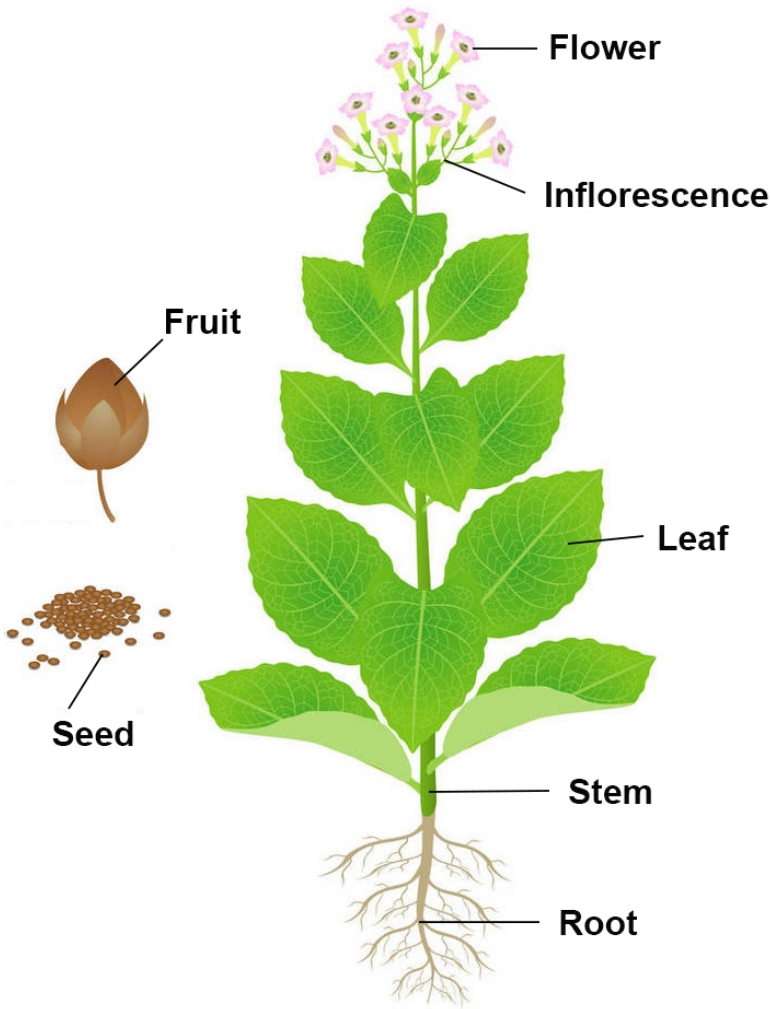

Fig. S16 The structural schematic drawing of *N. benthamiana* tissue.

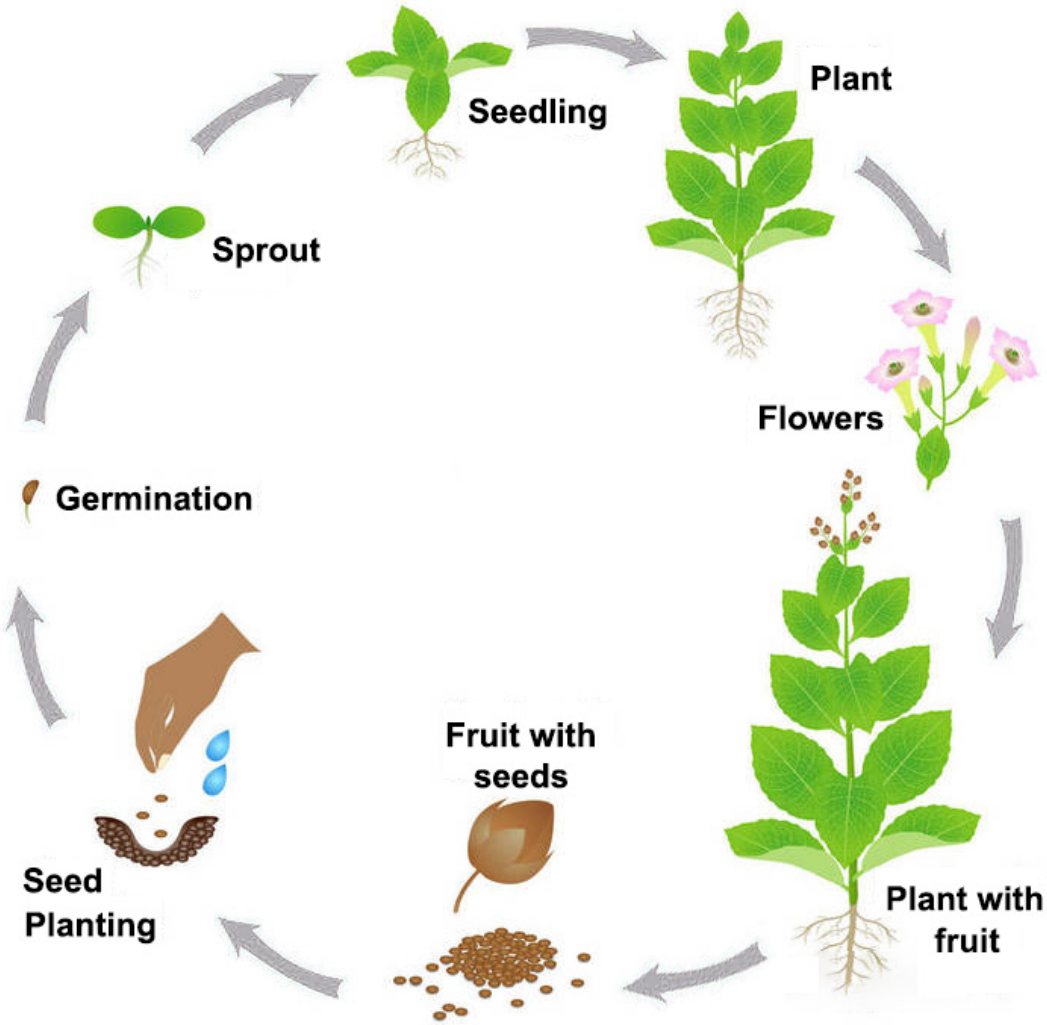

Fig. S17 The schematic process of planting, growth and maturity of *N. benthamiana* plant.

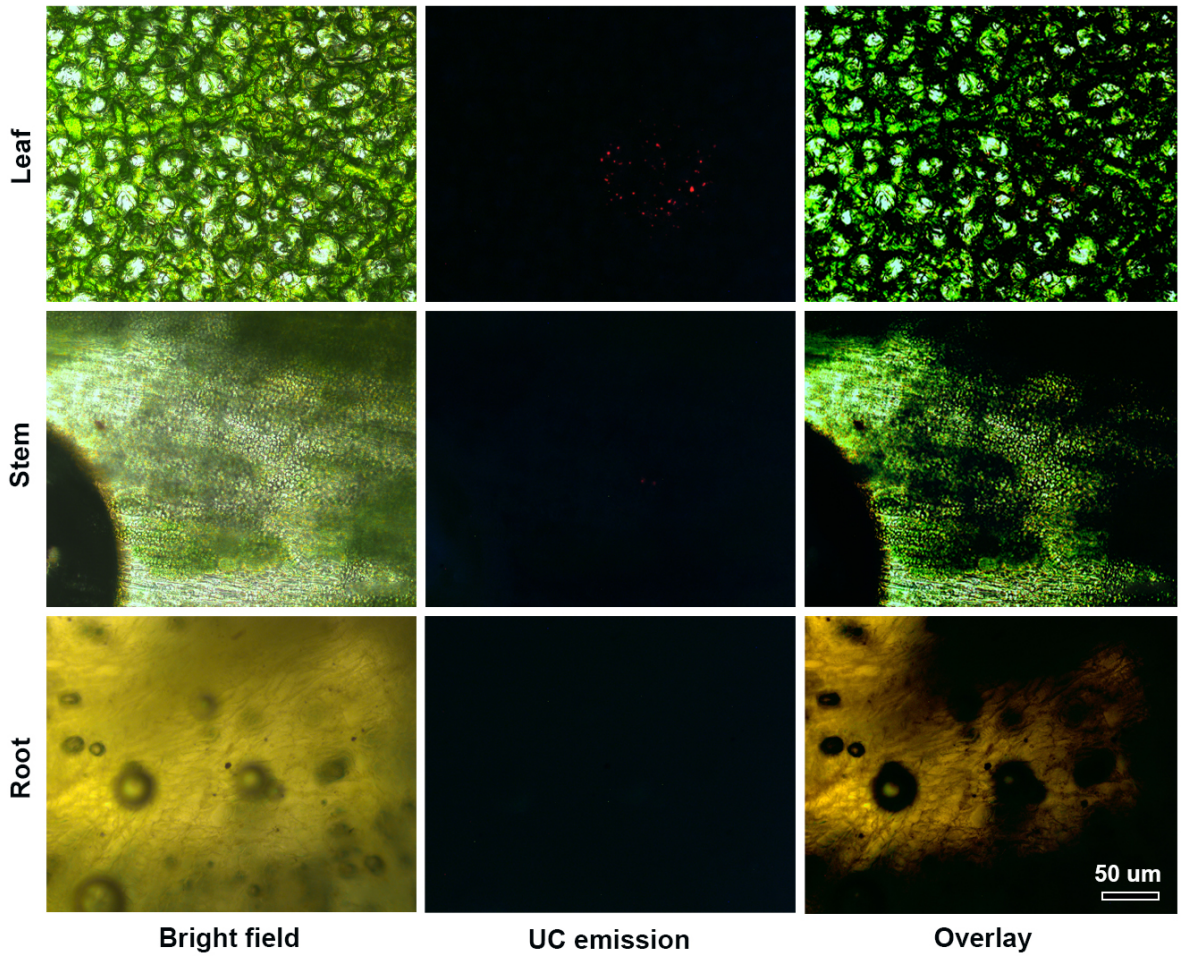

Fig. S18 Confocal microscopy images of transverse sections under 980 nm excitation from the leaf, stem, and root of *N. benthamiana*, sprayed with PEI-LDNPs for 7 days.

Table S1. The blood routines analysis data of obtained from mice fed with LDNPs at the 14th day (experiment) and mice receiving no feeding (control).

Test	Units	Control (mean ± sd)	Treatment (mean ± sd)
Hematological			
WBC	$\times 10^9$/L	5.7 ± 2.3	6.1 ± 2.2
NE	$\times 10^9$/L	11.9 ± 1.4	11.2 ± 1.3
LY	$\times 10^9$/L	68.9 ± 1.3	70.1 ± 1.1
RBC	$\times 10^{12}$/L	8.1 ± 1.7	9.6 ± 1.4
HGB	g/L	139.0 ± 14.2	141.1 ± 20.1
MCV	fL	40.7 ± 5.1	48.2 ± 3.4
MCH	pg	15.7 ± 1.9	17.6 ± 2.5
MCHC	g/L	370.6 ± 5.7	363.1 ± 9.8
RDW	%	20.9 ± 3.8	22.4 ± 2.7
PLT	$\times 10^9$/L	831.3 ± 68.6	840.5 ± 60.5